Biochemical and Biophysical Research Communications 436 (2013) 491–496

Contents lists available at SciVerse ScienceDirect

Biochemical and Biophysical Research Communications

journal homepage: www.elsevier.com/locate/ybbrc

An unusual mode of iron–sulfur-cluster coordination in a teleost glutaredoxin

Lars Bräutigam [a], Catrine Johansson [b], Bastian Kubsch [a], Michael A. McDonough [c], Eckhard Bill [d], Arne Holmgren [a,*], Carsten Berndt [a,e,*]

[a] Division for Biochemistry, Department for Medical Biochemistry and Biophysics, Karolinska Institutet, 17177 Stockholm, Sweden
[b] Structural Genomics Consortium, University of Oxford, Old Road Campus Research Building, Oxford OX3 7DQ, United Kingdom
[c] Chemistry Research Laboratory, Department of Chemistry, Oxford OX1 3TA, United Kingdom
[d] Max-Planck-Institute for Bioinorganic Chemistry, 45470 Mülheim/Ruhr, Germany
[e] Heinrich-Heine-University, Department of Neurology, Medical Faculty, Merowinger Platz 1a, 40225 Düsseldorf, Germany

ARTICLE INFO

Article history:
Received 29 May 2013
Available online 10 June 2013

Keywords:
Zebrafish
Crystal structure
Mössbauer spectroscopy
Redox
Glutathione

ABSTRACT

Glutaredoxins that contain a Cys-X-X-Cys active site motif are glutathione-dependent thiol-disulfide oxidoreductases. Vertebrate glutaredoxin 2 is characterized by two extra cysteines that form an intramolecular disulfide bridge. Zebrafish glutaredoxin 2 contains four additional cysteines that are conserved within the infraclass of bony fish (teleosts). Here, we present a biochemical and biophysical characterization of zebrafish glutaredoxin 2, focusing on iron–sulfur-cluster coordination. The coordination of $[2Fe2S]^{2+}$-clusters in monomers of this protein was revealed by both absorption and Mössbauer spectroscopy as well as size exclusion chromatography. All other holo-glutaredoxins represent [FeS]-cluster bridged dimers using two molecules of non-covalently bound glutathione and the N-terminal active site cysteines as ligands. These cysteine residues were not required for [FeS]-cluster coordination in zebrafish glutaredoxin 2. A crystal structure of the teleost protein revealed high structural similarity to its human homologue. The two vertebrate-specific cysteines as well as two of the teleost-specific cysteines are positioned within a radius of 7 Å near the C-terminus suggesting a potential role in [FeS]-cluster coordination. Indeed, mutated proteins lacking these teleost-specific cysteines lost the ability to bind the cofactor. Hence, the apparent mode of [FeS]-cluster coordination in zebrafish glutaredoxin 2 could be different from all yet described [FeS]-glutaredoxins.

1. Introduction

Glutaredoxins (Grxs) are glutathione (GSH)-dependent thiol-disulfide oxidoreductases that are known to function in the maintenance of cellular redox homeostasis and thiol-redox signaling *via* reduction of glutathionylated thiols or protein disulfides [1,2]. Grxs are characterized by a Cys-X-X-Cys active site motif and a common structure, the thioredoxin (Trx)-fold, comprised of a four stranded β-sheet surrounded by three to five α-helices [3].

A subfamily of Grxs lacking the C-terminal active site cysteine (Cys-X-X-Ser) and therefore named monothiol Grxs, has been discovered and investigated during the last decade [1,4]. Both monothiol and dithiol Grxs, have been characterized as [FeS]-cluster coordinating proteins in virtually all kingdoms of life [1,5,6]. [FeS]-clusters are inorganic cofactors with a variety of functions, mostly supporting electron transfer reactions, *e.g.* in proteins that are essential for life due to their importance in protein translation, nucleotide excision repair, and DNA replication [7–9]. In most proteins, [FeS]-clusters are coordinated *via* cysteine and/or histidine residues [10].

The group of [FeS]-cluster containing proteins was expanded to include Grxs in 2005 with the identification of human Grx2 as [FeS]-cluster coordinating enzyme [11]. In contrast to other [FeS]-proteins, holo-hGrx2 was found to be enzymatically inactive and to require a non-protein ligand, glutathione (GSH), for cluster coordination [11,12]. All available crystal structures of mono-, and dithiol Grxs indicate that these proteins bind a $[2Fe2S]^{2+}$-cluster bridged between two monomers *via* the N-terminal active site cysteines and two molecules of non-covalently bound GSH [13–17].

Abbreviations: Grx, glutaredoxin; GSH, glutathion; GSSG, glutathione disulphide; HED, hydroxyethyl disulphide; Trx, thioredoxin.

* Corresponding authors. Address: Division of Biochemistry, Department of Medical Biochemistry and Biophysics, Karolinska Institutet, Scheelesväg 2, SE-17177 Stockholm, Sweden (A. Holmgren), Heinrich-Heine-University, Department of Neurology, Medical Faculty, Merowinger Platz 1a, 40225 Düsseldorf, Germany (C. Berndt).

E-mail addresses: Arne.Holmgren@ki.se (A. Holmgren), Carsten.Berndt@ki.se (C. Berndt).

0006-291X/$ - see front matter © 2013 Elsevier Inc. All rights reserved.
http://dx.doi.org/10.1016/j.bbrc.2013.05.132

It was previously reported that monothiol [FeS]-cluster containing Grxs are involved in iron homeostasis [18,19] and [FeS]-cluster biosynthesis [5]. The [FeS]-cluster in dithiol Grxs may serve as redox sensor [12], as GSH in holo-Grxs is in constant exchange with free GSH, thereby connecting cluster stability to the cellular redox potential [11,12].

The human genome and that of other vertebrates encodes for two dithiol Grxs (Grx1 and Grx2) as well as two monothiol Grxs (Grx3 and Grx5) [1]. With the exception of Grx1, all human Grxs have been identified as [FeS]-cluster containing Grxs [11,16,20]. It was suggested that substitution of the proline residue in the consensus active site motif Cys-Pro-Tyr-Cys (Grx1) with another amino acid, *e.g.* serine as in Grx2, allows for the coordination of the [FeS]-cluster [12–14].

The gene encoding human Grx2 (hGrx2) gives rise to three different isoforms, each having distinct sub-cellular locations: hGrx2a in mitochondria and hGrx2b and 2c variants in nucleus and cytosol, respectively [21]. The homologue of hGrx2c in zebrafish, an important model organism for investigation of vertebrate embryonic development, is zebrafish Grx2 (zfGrx2). We recently demonstrated the essential function of zfGrx2 for embryonic brain development, as knock-down of zfGrx2 inhibited the formation of the axon scaffold and induced apoptotic cell death in developing neurons [22].

In this study we performed a biochemical and biophysical analysis of zfGrx2 with regard to its ability to coordinate a [FeS]-cluster.

2. Materials and methods

2.1. Protein expression and purification

Plasmids for the expression of zfGrx2 variants were generated by rolling circle PCR as described before [22], or by using the primer pairs listed in Table S1. Expression of recombinant protein was performed in auto-induction medium [23] using *Escherichia coli* BL21(DE3)pRIL (Stratagene) harboring the respective pET15b plasmid. The cultures were incubated at 37 °C for 1 h followed by 36 h at 18 °C, and the protein was purified as previously described [22]. The concentration of the enzyme was determined by spectroscopy using the A_{280nm} extinction coefficient of 3480 M^{-1} cm^{-1}.

For Mössbauer spectroscopy, bacteria were grown in iron-depleted Vogel–Bonner medium [24] until they reached an OD_{600} of 0.8. Together with 0.5 mM isopropyl β–D-thiogalactoside for induction of zfGrx2 expression, the medium was supplemented with 2 mg l^{-1} $^{57}FeCl_3$.

2.2. Oligomerisation analysis

The quarternary structure of zfGrx2 was analyzed by size exclusion chromatography. ZfGrx2 was applied to a Superdex G200 column (GE healthcare) equilibrated with 50 mM sodium phosphate, 300 mM NaCl, 10% glycerol, pH 8.0 and absorbance at 280 and 320 nm was recorded.

2.3. Bioinformatics

Primary sequence was analyzed with ClustalW [25] and blast2p.

2.4. Crystallization and data collection

For crystallization experiments, purified zfGrx2 was concentrated to 42 mg ml^{-1}. The protein was crystallized at 4 °C by the sitting drop vapor diffusion method (100 nl protein, 50 nl reservoir solution including 5 mM GSSG). Drops were equillibrated against 20 µl of reservoir solution containing 0.3 M $NaKC_4H_4O_6$, 2 M $(NH_4)_2SO_4$, 0.1 M $C_6H_5Na_3O_7$, pH 5.0. A single prism shaped crystal (approximately 50 × 100 × 270 µm) grew after six weeks and was transferred directly to the reservoir solution supplemented with 20% (v/v) glycerol and cryo-cooled in liquid nitrogen for storage and data collection.

2.5. Data collection and processing

Data were collected at 100 K using a Rigaku FRE+ SuperBright rotating copper anode X-ray generator equipped with varimax HF optics and a Saturn 944+ CCD detector. Data were integrated and scaled with the HKL2000 package [26]. Data collection statistics are summarized in Table S2. The data were indexed and scaled as trigonal space group *R*32 to 2.6 Å resolution.

2.6. Structure solution and refinement

The structure of zfGrx2 was solved by molecular replacement using PHASER [27] as implemented through PHENIX [28] using the hGrx2 structure (PDB ID 2FLS) as the search model. The initial electron density maps were of good quality and a model was built using COOT [29]. Iterative rounds of refinement and fitting were performed using PHENIX and COOT until convergence to a final R_{factor} and R_{free} of 18.9% and 25.0%, respectively. Refinement statistics are summarized in Table S2.

2.7. Determination of enzymatic activity

Enzymatic activity of zfGrx2 was measured using the hydroxyethyl disulfide (HED) assay [30]. Calculated kinetic constants are the result of three independent measurements.

2.8. Spectroscopy

UV–Vis spectra, as well as cluster and protein stability measurements were recorded with a Shimadzu UV-1200 spectrophotometer. Mössbauer spectroscopy was performed with alternating constant acceleration of the γ-source. The minimum experimental line width was 0.24 mm s^{-1} (full width at half-time). The temperature was kept constant using the Oxford Instruments Mössbauer Spectromag cryostat. Isomer shifts are quoted relative to metallic iron at 300 K. X-band EPR spectra were recorded with a Bruker Elexsys E500 spectrometer equipped with a helium flow cryostat (Oxford Instruments ESR 910), an NMR gaussmeter, and a Hewlett-Packard frequency counter.

3. Results

A gene encoding a protein homologous to hGrx2 was identified as zfGrx2 [31]. ZfGrx2 possesses a total of eight cysteine residues; two in the dithiol active site motif (Cys37 and Cys40), two vertebrate-specific cysteines (Cys28 and Cys113) that have been reported to establish an intra-molecular disulfide in hGrx2 [11,13], and four additional cysteine residues (Cys16, Cys90, Cys116 and Cys117) which are uniquely conserved in the teleost infraclass with as yet unknown function (Fig. S1). We determined the crystal structure of zfGrx2 to identify the positions of these extra cysteines in the hope that this would provide clues as to their biochemical function.

3.1. Crystal structure of zfGrx2

ZfGrx2 was crystallized aerobically in the presence of glutathione disulfide (GSSG) and the structure was determined to 2.6 Å resolution (PDB ID 3UIW). Two molecules are present in the

asymmetric unit (chains A and B) forming a crystallographic dimer which then associates with two symmetry related molecules by an inter-molecular disulfide formed between Cys116 in molecules A–A′ and B–B′ forming a crystallographic tetramer (Fig. 1A). The two molecules that make up the asymmetric unit are very similar having an overall root mean square deviation of 0.6 Å based on all Cα atoms.

The overall structure of zfGrx2 possesses a Trx-fold with a four stranded mixed beta-sheet flanked by five α-helices and is almost identical to that of hGrx2 (PDB ID 2FLS) (RMSD: 0.38 Å based on 84 Cα atoms) (Fig. 1B). A GSH molecule is bound to the conserved GSH binding site and has an almost identical orientation and interactions with the protein as observed for the structure of hGrx2 (Fig. 1B, Fig. S2). The GSH-glutamyl carboxylate forms hydrogen bonds to the backbone amides of Gly94 and Ser95 (2.8 Å). The GSH cysteinyl backbone nitrogen hydrogen bonds to the backbone carbonyl oxygen of Val81 (2.6 Å), and the GSH glycine carboxylate forms an electrostatic interaction with the side chain amine of Lys34 (2.7 Å) and hydrogen bonds to the side chain nitrogen of Gln69 (2.5 Å). The Cys-Pro-Tyr-Cys active site motif is located in the beginning of helix α-2, where Cys37 forms a mixed disulfide bond with the bound GSH (S–S bond distance 2.1 Å). The teleost-specific Cys16 is located at the beginning of helix α-1 and is exposed to the surface, whereas Cys90 is semi-buried and located at the end of strand β-4. Cys28 and Cys113, which are located at the beginning of strand β-1 and the end of helix α-5, respectively, form an intra-molecular disulfide which anchors the N- and C-terminus of the protein and is semi-buried at the interface between the crystallographic dimers (Fig. 1C). This disulfide bond is also present in hGrx2 where it preserves structural integrity [12,13]. Both Cys116 and Cys117 are located at the C-terminus of the protein. Cys116 forms a disulfide with Cys116 of a symmetry related molecule of the same chain but from a different asymmetric unit (i.e. A116-A′116/B116-B′116). Chain A Cys117, which is buried in the crystallographic dimer interface, is located 3.6–5.5 Å from the Cys28-Cys113 disulfide in the symmetry related molecule A′. In summary, four cysteines (Cys28, Cys113, Cys116 and Cys117) from a single chain of zfGrx2 are clustered within a 7 Å radius near the C-terminus (Fig. 1C). The absence of an [FeS]-cluster in the crystal structure is not unusual for Trx family members due to the high instability of such a complex under crystallization conditions. Thus, further biochemical and biophysical characterization was required to understand how zfGrx2 coordinates its [FeS]-cluster.

3.2. [FeS]-cluster coordination in zfGrx2

Recombinantly expressed and purified zfGrx2 appeared as yellow/brownish colored protein like other Grxs characterized as [FeS]-cluster coordinating proteins. As other [FeS]-Grxs, zfGrx2 displayed absorbance bands at 320 and 420 nm that are characteristic for proteins with a coordinated [2Fe2S]-cluster [10] (Fig. 2A). ZfGrx2 appeared as predominantly monomeric protein with an apparent mass of 19 kDa (calculated mass including His-tag: 17 kDa) by gel filtration chromatography (Fig. 2B, Fig. S3A). Surprisingly, both the monomeric and dimeric form showed absorbance at 320 nm. This suggested that in contrast to all yet described [FeS]-Grxs, the [FeS]-cluster can be coordinated by monomeric zfGrx2.

To determine the ligands necessary for [FeS]-cluster coordination, we investigated several cysteine to serine variants regarding their ability to bind the cofactor. ZfGrx2C37S, lacking the N-terminal active site cysteine essential for [FeS]-cluster coordination in all other Grxs, showed no difference in the ability to coordinate the cluster compared to its wildtype counterpart (Fig. 2A and B). Mutation of the teleost specific Cys16 and Cys90, as well as the exchange of the C-terminal active site Cys40 to serines did not alter the spectral properties characteristic for the presence of an [FeS]-cluster (Fig. 2C). Surprisingly, the variants lacking either or both of the teleost-specific residues Cys116 and Cys117 at the C-terminus lost the ability to coordinate the chromophore in both the monomer and dimer fractions (Fig. 2D and E). Cys116 and Cys117 are in close spatial proximity to Cys28, one of the cysteine residues forming an intra-molecular disulfide in zfGrx2. Substitution of Cys28 to a serine abolished the ability of zfGrx2 to bind the [FeS]-cluster (Fig. 2F). However, loss of the [FeS]-cluster in zfGrx2C28S may be due to the increased protein instability, as observed in hGrx2 [13] (Fig. 2G).

In addition to UV/VIS spectroscopy, the coordination of a [2Fe2S]-cluster in zfGrx2 was confirmed by zero-field Mössbauer spectroscopy measurements (Fig. 2H). The same protein used for Mössbauer spectroscopy was also applied to gel-filtration and appeared mainly as monomeric protein as described before (Fig. S3B). The spectrum recorded at 80 K showed an asymmetric Lorentzian doublet consisting of two subspectra. The main species (subspectrum I, 72% abundance) had an isomer shift of $\delta = 0.29$ mm s^{-1}, a quadrupole splitting of $\Delta E_Q = 0.40$ mm s^{-1}, and a Lorentzian line width of $\Gamma_{fwhm} = 0.41$ mm s^{-1}. The Mössbauer parameters of this predominant subspectrum are characteristic for Fe^{III} in tetrahedral

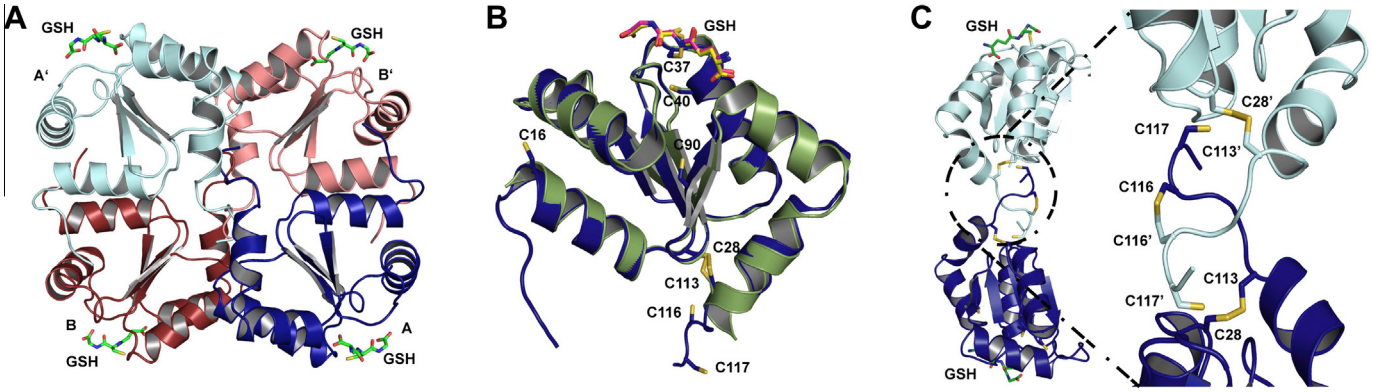

Fig. 1. Crystal structure of zfGrx2 (PDB ID 3UIW). (A) The two molecules in the asymmetric unit (A and B, dark blue and brick red) form a crystallographic tetramer with two symmetry related molecules (A′ and B′, cyan and pink) *via* a Cys116 inter-molecular disulfide bridge. (B) Superposition of zfGrx2 (dark blue) with hGrx2 (light green, PDB ID 2FLS). The GSH molecules are shown as sticks colored yellow (zfGrx2) and magenta (hGrx2). (C) Ribbon representation of the crystallographic dimer formed between two symmetry related molecules (A and A′) with a close up view of the dimer interface.

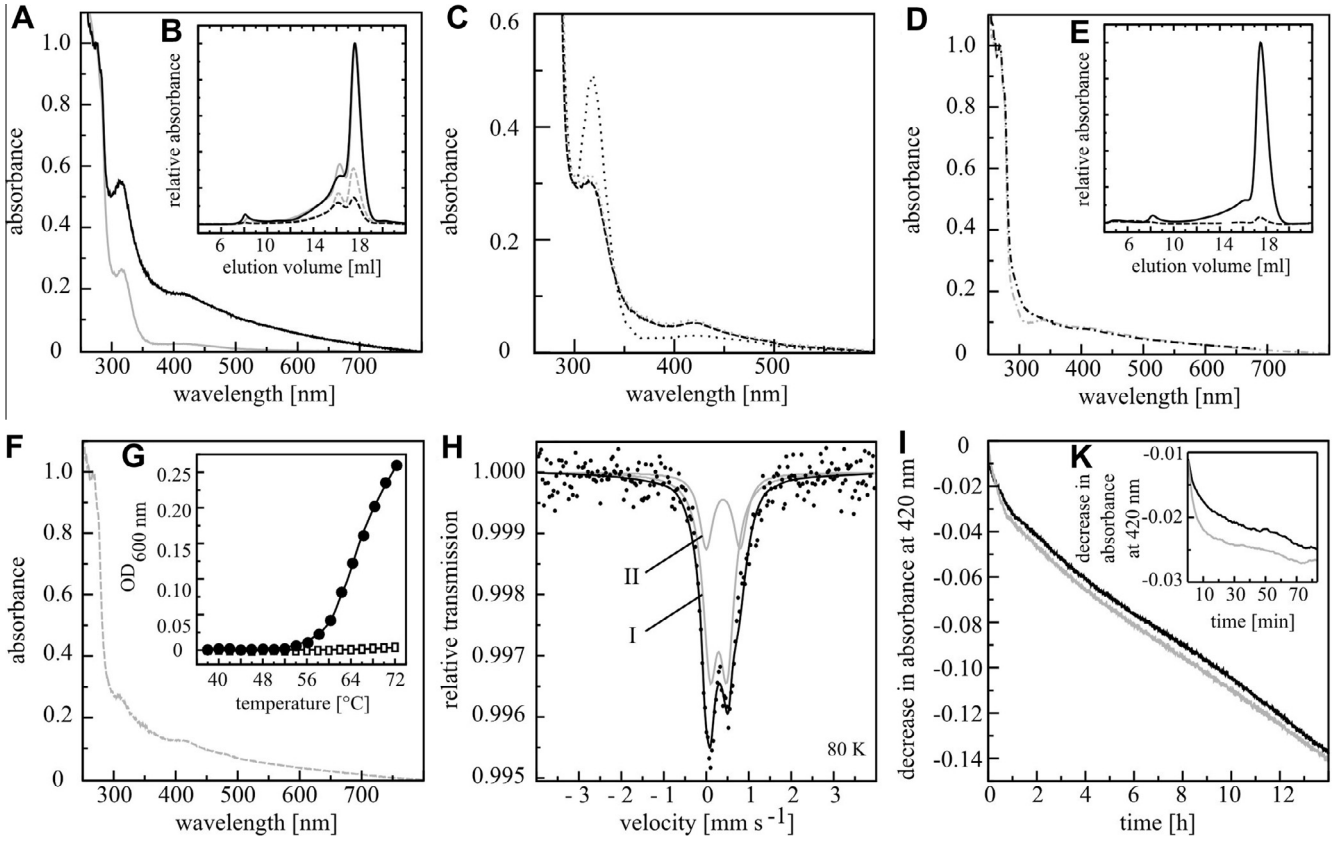

Fig. 2. ZfGrx2 monomers coordinate a $[2Fe2S]^{2+}$-cluster. (A) UV–Vis spectra of freshly purified zfGrx2 (solid, black) and zfGrx2C37S (solid, gray) indicate coordination of an [FeS]-cluster by absorbance at 320 and 420 nm. (B) Elution profiles of zfGrx2 (black) and zfGrx2C37S (gray) (280 nm: solid, 320 nm: dashed) separated by a Superdex G200 column. (C) UV–Vis spectra of zfGrx2C16S (dashed, black), zfGrx2C40S (dotted, gray), zfGrx2C90S (dotted, black). (D) UV–Vis spectra of zfGrx2C116S (dashed/dotted, gray), zfGrx2C117S (dashed/dotted, black). (E) Elution profile of zfGrx2C116/117S (280 nm: solid, 320 nm: dashed). (F) UV–Vis spectra of zfGrx2C28S (dashed, gray). (G) Protein stability measured as turbidity at indicated temperatures of zfGrx2 (white squares) and zfGrx2C28S (black circles). (H) Zero-field Mössbauer spectroscopy of zfGrx2 (1.4 mM) recorded at 80 K. Dots represent the measuring points which are the base for the calculated Lorentzian doublet (black line) consisting of two subspectra (gray lines). (I, K) [FeS]-cluster stability was measured following decrease in absorbance at 420 nm upon exposure to air (I) and 0.5 mM dithionite (K) at 25 °C without (black) or with 2 mM GSH (gray). UV–Vis spectra were normalized to absorbance at 276 nm. For molecular mass calibration see Fig. S2.

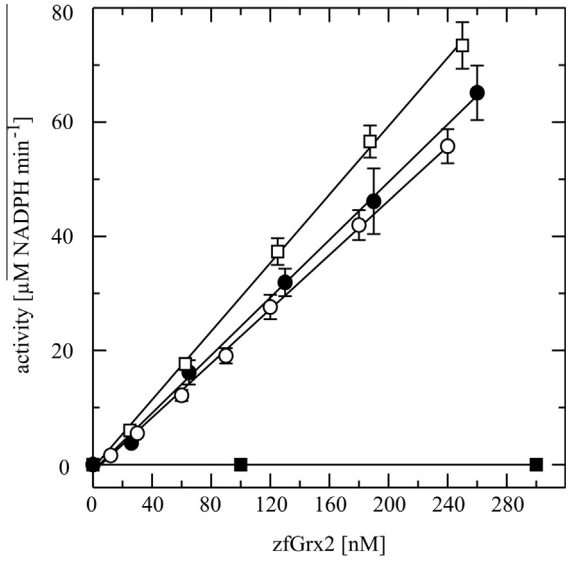

Fig. 3. Enzymatic activity of zfGrx2. Activity measurements of zfGrx2 after purification (black circles, *kcat* s^{-1} = 4.24 ± 0.36) and after [FeS]-cluster removal following dithionite treatment (white squares, *kcat* s^{-1} = 4.50 ± 0.26), zfGrx2C37S (black squares, not active) and zfGrx2C116/117S (white circles, *kcat* s^{-1} = 3.36 ± 0.28) were determined by HED assays.

sulfur coordination. Additional experiments have shown that the cluster was silent in electro-paramagnetic resonance spectroscopy (data not shown). The combination of EPR and Mössbauer data strongly suggests the presence of a dinuclear $[2Fe2S]^{2+}$-cluster with coupled spins and ground state $S = 0$ coordinated by four cysteine residues in zfGrx2. Subspectrum II (28% abundance) with $\delta = 0.40$ mm s^{-1}, $\Delta E_Q = 0.80$ mm s^{-1}, and $\Gamma_{fwhm} = 0.38$ mm s^{-1} most likely arose from non-protein bound Fe^{3+} aggregates (Fig. 2H).

Although the crystal structure of zfGrx2 demonstrated that GSH binds in a similar fashion compared to hGrx2 [13], GSH did not support stability of the [FeS]-cluster during exposure to air (Fig. 2K) or dithionite (Fig. 2L). The above presented results suggest that the [FeS]-cluster is not bound by the active site cysteine and should therefore not inhibit enzymatic activity of the holo-protein. Indeed, compared to the *kcat* $s^{-1}$of 4.24 ± 0.36 of holo-zfGrx2 directly after purification, which is in the range of mammalian apo-Grx2s [12], the enzymatic activity of zfGrx2 did not change significantly after removal of the [FeS]-cluster with dithionite (*kcat* s^{-1} of 4.50 ± 0.26). The determined activity of zfGrx2C116/117S (*kcat* s^{-1} of 3.36 ± 0.28) was similar to wildtype protein, whereas zfGrx2C37S was, as expected, not active (Fig. 3).

4. Discussion

Dithiol Grxs are characterized by the Trx-fold and the presence of a Cys-X-X-Cys active site [1]. Although this motif is well known

for the coordination of metals in a variety of proteins, not all members of the Trx family are [FeS]-proteins [32]. Features inhibiting metal coordination are the presence of the *cis*-proline [33] and the proline residue, located within the consensus active site motif Cys-Pro-Tyr-Cys [12–14]. Variants of Grxs and Trx1 in which a proline within the active site was replaced or introduced, gained or lost the ability to coordinate the chromophore, respectively [12,14,34]. However, recently the first [FeS]-Grx with the consensus active site motif has been identified [35]. Independent of the primary active site sequence, all analyzed [FeS]-Grxs coordinate the cluster *via* the N-terminal active site cysteines of two protomers inhibiting enzymatic activity of the holo-protein [1]. The other ligand is contributed by the thiols of non-covalently bound GSH [1]. GSH is in constant exchange with surrounding GSH and high GSH concentrations are thereby stabilizing holo-Grxs [12,14]. All these Grx-specific characteristics of [FeS]-cluster binding are not observed in zfGrx2.

Surprisingly, the presence of an [2Fe2S]-cluster was not limited to zfGrx2 dimers. In contrast to its human homologue, freshly purified holo-zfGrx2 was enzymatically active, not stabilized by GSH, and its N-terminal active site variant C37S retained the spectral properties of a [FeS]-cluster protein. Thus, it is possible that the proline in the consensus active site of zfGrx2 prevents [FeS]-cluster coordination. Substitution of this proline makes the structure more flexible [13], whereas the proline present in the zfGrx2 active site may interfere with [FeS]-cluster coordination (Fig. S4). We demonstrated that the teleost-specific cysteine residues Cys116 and Cys117 as well as the vertebrate-specific Cys28 are important for [FeS]-cluster coordination in zfGrx2. The crystal structure of apo-zfGrx2 revealed that these cysteines are in close proximity to Cys113. The inter-molecular disulfide formed between Cys116 of two asymmetry related molecules is likely to be a crystallographic artifact, whereas the intra-molecular disulfide formed between Cys28 and Cys113 appears to be conserved in vertebrates. As previously been shown by NMR spectroscopy, the C-termini of Grxs are very flexible [36,37]. Therefore, the formation of an environment allowing the coordination of an [FeS]-cluster by the four cysteines in the monomeric protein is possible. However, in order to coordinate the cofactor the structural disulfide has to be reduced. This has recently been observed in the structure of the first Grx-domain of hGrx3, with cysteines in similar but not identical positions (PDB ID 3ZYU, Johansson et al., manuscript in preparation). Thus, it may be possible that zfGrx2, and potentially homologues from other teleostei, may be able to coordinate an [FeS]-cluster using the four sulfhydryl residues Cys28, Cys113, Cys116 and Cys117 (Fig. 4).

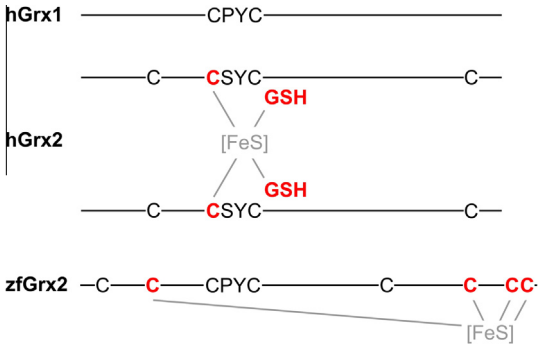

Fig. 4. Proposed [FeS]-cluster coordination of zfGrx2. In comparison to human Grx1, which is not able to coordinate an [FeS]-cluster and hGrx2 that uses the N-terminal active site cysteines and GSH as ligands to form an [FeS]-cluster bridged dimer (representing the so far only identified mode of cofactor coordination in Grxs), zfGrx2 uses potentially four cysteines to coordinate an [FeS]-cluster in monomers. Cysteine residues suggested as ligands are marked.

The cysteines that likely coordinate the [FeS]-cluster in zfGrx2 are present in all yet identified teleost homologues (Fig. S1). Our study indicates that various undetected modes of [FeS]-cluster coordination in Grxs may exist and might have been established independently during evolution. Cluster coordination in zfGrx2 seems to be a cross between Grxs and ferredoxins. The [2Fe2S]-cluster in *Aquifex aeolicus* ferredoxin, which was recently recognized as Trx-fold protein, is coordinated by four cysteines located near the site corresponding to that of the active site in Trxs and Grxs [38].

In summary, we provide evidence that zfGrx2 may bind an [FeS]-cluster using an alternative coordination mode when compared to all other [FeS]-Grxs described. Additional studies are needed to further elucidate the details of how these cysteines are able to coordinate the [2Fe2S]-cluster and to investigate the function of this cluster in bony fish.

Acknowledgments

We thank Nina Voevodskaya (Stockholm University, EPR spectroscopy), Bernd Mienert (Max-Planck-Institute, Mülheim/Ruhr, Mössbauer spectroscopy), and Tomas Gustafsson (Karolinska Institutet, protein expression). This work was supported by German Research Society, Karolinska Institutet, Swedish Cancer Society, the K.A. Wallenberg Foundation, and Swedish research Council.

Appendix A. Supplementary data

Supplementary data associated with this article can be found, in the online version, at http://dx.doi.org/10.1016/j.bbrc.2013.05.132.

References

[1] C.H. Lillig, C. Berndt, A. Holmgren, Glutaredoxin systems, Biochim. Biophys. Acta 1780 (2008) 1304–1317.
[2] C.H. Lillig, C. Berndt, Glutaredoxins in thiol/disulfide exchange, Antioxid. Redox Signal. 18 (2012) 1654–1665.
[3] A. Holmgren, Thioredoxin structure and mechanism: conformational changes on oxidation of the active-site sulfhydryls to a disulfide, Structure 3 (1995) 239–243.
[4] M.T. Rodríguez-Manzaneque, J. Ros, E. Cabiscol, et al., Grx5 glutaredoxin plays a central role in protection against protein oxidative damage in *Saccharomyces cerevisiae*, Mol. Cell. Biol. 19 (1999) 8180–8190.
[5] N. Rouhier, J. Couturier, M. Johnson, et al., Glutaredoxins: roles in iron homeostasis, Trends Biochem. Sci. 35 (2010) 43–52.
[6] A. Picciocchi, C. Saguez, A. Boussac, et al., CGFS-type monothiol glutaredoxins from the cyanobacterium *Synechocystis* PCC6803 and other evolutionary distant model organisms possess a glutathione-ligated [2Fe-2S] cluster, Biochemistry 46 (2007) 15018–15026.
[7] G. Kispal, K. Sipos, H. Lange, et al., Biogenesis of cytosolic ribosomes requires the essential iron-sulphur protein Rli1p and mitochondria, EMBO J. 24 (2005) 589–598.
[8] J. Rudolf, V. Makrantoni, W.J. Ingledew, et al., The DNA repair helicases XPD and FancJ have essential iron-sulfur domains, Mol. Cell 23 (2006) 801–808.
[9] S. Klinge, J. Hirst, J.D. Maman, et al., An iron-sulfur domain of the eukaryotic primase is essential for RNA primer synthesis, Nat. Struct. Mol. Biol. 14 (2007) 875–877.
[10] H. Beinert, R.H. Holm, E. Münck, Iron-sulfur clusters: nature's modular, multipurpose structures, Science 277 (1997) 653–659.
[11] C.H. Lillig, C. Berndt, O. Vergnolle, et al., Characterization of human glutaredoxin 2 as iron–sulfur protein: a possible role as redox sensor, Proc. Natl. Acad. Sci. U.S.A. 102 (2005) 8168–8173.
[12] C. Berndt, C. Hudemann, E.M. Hanschmann, et al., How does iron-sulfur cluster coordination regulate the activity of human glutaredoxin 2?, Antioxid Redox Signal. 9 (2007) 151–157.
[13] C. Johansson, K.L. Kavanagh, O. Gileadi, et al., Reversible sequestration of active site cysteines in a 2Fe-2S-bridged dimer provides a mechanism for glutaredoxin 2 regulation in human mitochondria, J. Biol. Chem. 282 (2007) 3077–3082.
[14] N. Rouhier, H. Unno, S. Bandyopadhyay, et al., Functional, structural, and spectroscopic characterization of a glutathione-ligated [2Fe-2S] cluster in poplar glutaredoxin C1, Proc. Natl. Acad. Sci. U.S.A. 104 (2007) 7379–7384.
[15] T. Iwema, A. Picciocchi, D.A. Traore, et al., Structural basis for delivery of the intact [Fe2S2] cluster by monothiol glutaredoxin, Biochemistry 48 (2009) 6041–6043.

[16] C. Johansson, A.K. Roos, S.J. Montano, et al., The crystal structure of human GLRX5: iron-sulfur cluster co-ordination, tetrameric assembly and monomer activity, Biochem. J. 433 (2011) 303–311.
[17] J. Couturier, C.S. Koh, et al., Structure-function relationship of the chloroplastic glutaredoxin S12 with an atypical WCSYS active site, J. Biol. Chem. 284 (2009) 9299–9310.
[18] U. Mühlenhoff, S. Molik, J.R. Godoy, et al., Cytosolic monothiol glutaredoxins function in intracellular iron sensing and trafficking via their bound iron-sulfur cluster, Cell Metab. 12 (2010) 373–385.
[19] H. Li, C.E. Outten, Monothiol CGFS glutaredoxins and BolA-like proteins: [2Fe-2S] binding partners in iron homeostasis, Biochemistry 51 (2012) 4377–4389.
[20] P. Haunhorst, C. Berndt, S. Eitner, et al., Characterization of the human monothiol glutaredoxin 3 (PICOT) as iron-sulfur protein, Biochem. Biophys. Res. Commun. 394 (2010) 372–376.
[21] M.E. Lönn, C. Hudemann, C. Berndt, et al., Expression pattern of human glutaredoxin 2 isoforms: identification and characterization of two testis/cancer cell-specific isoforms, Antioxid. Redox Signal. 10 (2008) 547–557.
[22] L. Bräutigam, L.D. Schütte, J.R. Godoy, et al., Vertebrate-specific glutaredoxin is essential for brain development, Proc. Natl. Acad. Sci. U.S.A. 108 (2011) 20532–20537.
[23] F.W. Studier, Protein production by auto-induction in high density shaking cultures, Protein Expr. Purif. 41 (2005) 207–234.
[24] H.J. Vogel, D.M. Bonner, Acetylornithinase of *Escherichia coli*: partial purification and some properties, J. Biol. Chem. 218 (1956) 97–106.
[25] M.A. Larkin, G. Blackshields, N.P. Brown, et al., Clustal W and clustal X version 2.0, Bioinformatics 23 (2007) 2947–2948.
[26] Z. Otwinowski, W. Minor, Macromolecular Crystallography, Part A, in: C.W. Carter, R.M. Sweet (Eds.), Methods in Enzymology, vol. 276, Academic Press, Waltham, 1997, pp. 307–326.
[27] A.J. McCoy, R.W. Grosse-Kunstleve, P.D. Adams, et al., Phaser crystallographic software, J. Appl. Crystallogr. 40 (2007) 658–674.
[28] P.D. Adams, P.V. Afonine, G. Bunkoczi, et al., PHENIX: a comprehensive Python-based system for macromolecular structure solution, Acta Crystallogr. D Biol. Crystallogr. 66 (2010) 213–221.
[29] P. Emsley, K. Cowtan, Coot: model-building tools for molecular graphics, Acta Crystallogr. D Biol. Crystallogr. 60 (2004) 2126–2132.
[30] M. Luthman, A. Holmgren, Glutaredoxin from calf thymus. Purification to homogeneity, J. Biol. Chem. 257 (1982) 6686–6690.
[31] J. Sagemark, T.H. Elgan, T.R. Bürglin, et al., Redox properties and evolution of human glutaredoxins, Proteins 68 (2007) 879–892.
[32] C.H. Lillig, C. Berndt, Thioredoxins and glutaredoxins. Functions in metal ion interactions, in: A. Sigel, H. Sigel, R.K.O. Sigel (Eds.), Metal Ions in Life Sciences 5, The Royal Society of Chemistry, Cambridge, 2009, pp. 413–439.
[33] D. Su, C. Berndt, D.E. Fomenko, et al., A conserved cis-proline precludes metal binding by the active site thiolates in members of the thioredoxin family of proteins, Biochemistry 46 (2007) 6903–6910.
[34] L. Masip, J.L. Pan, S. Haldar, et al., An engineered pathway for the formation of protein disulfide bonds, Science 303 (2003) 1185–1189.
[35] S. Ceylan, Y. Seidel, N. Ziebart, et al., The dithiol glutaredoxins of african trypanosomes have distinct roles and are closely linked to the unique trypanothione metabolism, J. Biol. Chem. 285 (2010) 35224–35237.
[36] M. Fladvad, M. Bellanda, A.P. Fernandes, et al., Molecular mapping of functionalities in the solution structure of reduced Grx4, a monothiol glutaredoxin from *Escherichia coli*, J. Biol. Chem. 280 (2005) 24553–24561.
[37] Y. Feng, N. Zhong, N. Rouhier, et al., Structural insight into poplar glutaredoxin C1 with a bridging iron-sulfur cluster at the active site, Biochemistry 45 (2006) 7998–8008.
[38] A.P. Yeh, C. Chatelet, S.M. Soltis, et al., Structure of a thioredoxin-like [2Fe-2S] ferredoxin from *Aquifex aeolicus*, J. Mol. Biol. 300 (2000) 587–595.